INFLUENCE OF SOLAR WIND STREAM INTERACTION REGIONS ON THE PROTON EVENT ON AUGUST 27, 2022

© 2025 N. A. Vlasova[a, *], G. A. Bazilevskaya[b], E. A. Ginzburg[c], E. I. Daibog[a], A.V. Dmitriev[a], V. V. Kalegaev[a,d], K. B. Kaportseva[a,d], Yu. I. Logachev[a], I. N. Myagkova[a], A.V. Suvorova[a]

[a]*Lomonosov Moscow State University, Skobeltsyn Institute of Nuclear Physics Moscow, Russian Federation*

[b]*Lebedev Physical Institute, Russian Academy of Sciences, Moscow, Russian Federation*

[c]*Fedorov Institute of Applied Geophysics, Moscow, Russian Federation*

[d]*Lomonosov Moscow State University, Faculty of Physics, Moscow, Russian Federation*

**e-mail: nav19iv@gmail.com*

Received March 20, 2025

Revised May 12, 2025

Accepted May 22, 2025

Abstract. The influence of large-scale interplanetary structures on the propagation of solar energetic particles on August 27, 2022 is studied. The dynamics of particles fluxes, observed at the Lagrange point L1 and in near-Earth space, has a number of features: the presence of synchronous local maxima of electron and proton fluxes of different energies during the flux growth phase; anisotropy of the solar proton flux for about 12 hours; the time profiles of solar protons observed near the Earth is similar to those observed at L1 point, but with a delay of more than 1 hour. It is proposed that the observed features can be explained by modulation processes during the propagation of particles inside the leading compression region ahead of the high-speed solar wind stream from the coronal hole.

Keywords: *solar flare, coronal mass ejection, coronal hole, solar wind, interplanetary magnetic field, solar energetic particles*

DOI: 10.31857/S00167940250501e2

1. INTRODUCTION

The rise of solar energetic proton fluxes, called the solar proton event (SPE), is not only of scientific interest in itself as a physical phenomenon, but also serves as a tool for studying processes on the Sun, in the interplanetary medium, and in the Earth's magnetosphere (e.g., [Lyubimov, 2003; Tverskaya, 2011]). The energy range of SPS particles (approximately from 1 MeV to several hundred MeV) determines the spatial and temporal scales of physical processes in the heliosphere, which can have a significant impact on the dynamics of particle fluxes. The interplanetary medium is inhomogeneous and nonstationary, and its structure can be represented differently on different spatial and temporal scales [Allen et al., 2023]. In space physics, the dynamics of processes on medium scales is of fundamental importance: in the solar wind, studies of processes on scales from 100 R_E (R_E is the Earth's radius) to a few degrees in heliolongitude at a distance of 1 a.u. (a.u. is an astronomical unit) are crucial to understanding the coupling between the Sun's corona and an observer at any point in the heliosphere [Allen et al., 2023]. It is on this spatial scale that the main structures of the interplanetary medium, such as interplanetary coronal mass ejections (ICMEs) and regions of interaction between fast and slow solar wind streams, fall, which can have the strongest impact on the flux of solar energetic particles during their propagation in the interplanetary medium and, thus, on the formation of the temporal profile of the SPS. The study of the SPS features allows us to visualize the substructure of these large-scale structures (e.g., [Tan et al., 2012; Lyubimov et al., 1976]).

Already experimental data from the Pioneer 6 spacecraft on variations in the anisotropy of solar particle fluxes correlating with changes in the direction and magnitude of the interplanetary magnetic field were interpreted as the motion of particles in the magnetic field filaments [McCracken and Ness, 1966]. The magnetic field fibers were depicted as tubes with a diameter of $3\cdot 10^6$ km [Bartleyr et al., 1966]. According to the results of the study also of the anisotropy of solar proton fluxes based on experimental data from the Mars-4, 5, 7 automatic interplanetary stations (AMS) – structures called magnetoplasma tubes with diameters of the order of 10^6 km were detected [Lyubimov et al., 1976]. The results of the study of experimental data obtained on the GRANAT spacecraft allowed us to detect bundles of magnetoplasma tubes [Ermakov et al., 1991]. In [Borovsky et al., 2008], an image of the interplanetary medium in the form of a magnetic carpet consisting of magnetic flux tubes differing in size and orientation in space was proposed. Thin current layers form the boundaries of magnetic flux tubes and separate one tube from another [Borovsky, 2018]. The origin of such heliospheric magnetic structure is unknown: either the structure has its source on the Sun or is formed in the solar wind itself [Neugebauer and Giacalone, 2015]. The surface of the Sun appears as a pattern consisting of granules and supergranules. In

[Mazur et al., 2000], it was suggested that the observed variations in the solar particle fluxes are due to the motions of the interplanetary magnetic field lines, which have as their source a network of supergranulations of the Sun's photosphere. At the same time, in [Khabarova et al., 2021], based on the study of current layers in the heliosphere, the possibility of the existence of a solar wind structure consisting of magnetic flux tubes, as suggested in [Borovsky, 2008; 2018], and the connection of such a structure with solar supergranulation is questioned. But it is pointed out that large quasi-stationary flux tubes do exist in large structures, such as the MCWM and the regions of interaction between fast and slow solar wind streams, as confirmed by various methods, including remote observations [Khabarova et al., 2021].

The fast solar wind stream, propagating in the heliosphere after a lower velocity stream, forms an interaction region with denser, compressed plasma in front of it (reviewed in [Richardson, 2018] and references therein). If a fast solar wind stream exists for more than one Carrington revolution of the Sun, it is said to form a corotating interaction region that can be observed for long periods of time. The existence of several interaction regions or corotating interaction regions in heliospheric space, their interaction with each other and/or with the MCWM leads to the formation of merged interaction regions (e.g., [Burlaga et al., 2003]).

The aim of this work is to determine the reasons for the formation of the complex temporal profile of solar energetic proton fluxes on 27.08.2022, based on the results of the analysis of solar energetic particle sources and conditions in the interplanetary medium during particle propagation.

2. SOURCES OF EXPERIMENTAL DATA

The study of the time profiles of solar proton fluxes on 08/27/2022 is based on experimental data obtained from spacecraft (SC) located in interplanetary space and in the Earth's magnetosphere. GOES-16 satellite is a geostationary Earth satellite. The data of measurements of solar proton fluxes with energies >5, >10, >30 and >60 MeV obtained from the *Solar and Galactic Proton Sensor (SGPS)* instrument (https://www.ngdc.noaa.gov/stp/satellite/goes-r.html) were used in this work. The ACE and DSCOVR satellites are located at the *L1* libration point, 1.5 million km from Earth (https://cdaweb.gsfc.nasa.gov/).

Electronic resources from which the information necessary for the study was obtained:

- on solar flares and coronal holes (https://www.solarmonitor.org/; https://www.spaceweatherlive.com/);
- on coronal mass ejections (CMEs) from the LASCO/C2 coronagraph on the SOHO spacecraft (https://cdaw.gsfc.nasa.gov/CME_list/);
- on images of the Sun at different wavelengths from SDO (https://www.solarmonitor.org/);

- solar wind and interplanetary magnetic field from the ACE and DSCOVR satellites (https://swx.sinp.msu.ru/);

- on solar energetic particle fluxes from ACE spacecraft and GOES-16 satellite (https://swx.sinp.msu.ru/).

Most of the figures in this paper were created on the website of the Operational Space Monitoring Data Center (OSMC) of the Moscow State University Research Institute of Nuclear Physics, which provides access to operational data of space experiments and models of operational forecasting of space weather phenomena. The CDOCM website in the section "Space Weather" (https://swx.sinp.msu.ru/) contains data necessary for assessing and analyzing the radiation situation not only in near-Earth space but also in the interplanetary environment. Electronic interactive versions of the catalogs of solar proton events of the 24th and 25th solar activity cycles and links to printed versions of the SPS catalogs of the 20th-24th solar activity cycles are also presented there (https://swx.sinp.msu.ru/apps/sep_events_cat/index.php?gcm=1&lang=ru).

3. EXPERIMENTAL RESULTS

The solar proton event on 27.08.2022 is associated with an explosive process on the Sun in the active region (AR) 13088. Two manifestations of this process are the solar flare of X-ray class M4.88 with heliocoordinates S17W79, which began at 01:52 UT, and a fast (velocity - 1284 km/s) with a wide solution angle (360°) coronal mass ejection (CME) registered at 02:24 UT (SPS catalog of the 25th solar activity cycle (https://swx.sinp.msu.ru/)). The solar flare was prolonged: onset at 01:52 UT, maximum at 02:40 UT, and end at 03:05 UT (https://www.spaceweatherlive.com/) (Fig. *1a*). In Fig. *1b*, along with the temporal profiles of solar proton fluxes, the electron flux profile from the ACE measurements is shown. The beginning of the electron flux increase at the *L1* point is observed approximately 1.5 ~~h~~ after the flare onset. The maximum flux of solar protons with $E > 10$ MeV during the event according to the GOES-16 satellite data was~ 27 $(cm^2\ s\ sr)^{-1}$ (Fig. *1c*). One of the features of SPS 27.08 is the presence of several local maxima in the growth phase of the solar particle fluxes (Fig. *1b* and Fig. *1c*). According to ACE data, the local maxima (Fig. *1b*, moments 1, 2, and 3) are observed simultaneously both for protons of different energies and electrons. Similar proton flux profiles with local maxima and also without energy dispersion can be seen in the GOES-16 data (Fig. *1c*). The only difference is the delay in the arrival of the fluxes in the region of the geostationary orbit compared to the Lagrangian point *L1* for more than 1 hour (Fig. *1c* - moments 1', 2', and 3').

Fig. 1.

The Meteor-M2 low-orbit polar satellite registered another feature of the SPS on 27.08.2022: the north-south asymmetry of proton fluxes with energies of 1-100 MeV. Figure *2a* shows the time profile of the proton flux during approximately one revolution of the satellite around the Earth. The efficiency of penetration of solar particles into the Earth's magnetosphere depends on many factors. First of all, on the orientation of the interplanetary magnetic field, the level of perturbation of the magnetosphere, and the energy of the particles (e.g., the work [Kuznetsov & Tverskaya, 2007] and references therein). Within the framework of this study, the problems of penetration of solar protons into the Earth's magnetosphere are not discussed in detail. Usually, the level of the particle flux in the polar caps corresponds to the flux in the interplanetary medium, but in a number of PCAs there is a north-south asymmetry of the fluxes, as can be seen in Fig. *2a* (the regions of the polar caps are highlighted by rectangles, the flux in the southern polar cap is higher than in the northern one). On 08/27/2022, the asymmetry of particle fluxes in near-Earth space was observed from~ 08 UT, from the time when the solar proton flux exceeded the background level, until~ 22 UT. The asymmetry of the solar proton fluxes was first recorded in November 1967 and, just like on 08/27/2022, the flux in the southern cap exceeded the flux in the northern cap for quite a long time,~ 20 h [Evans and Stone, 1969]. The different flux of solar particles in the polar caps is explained by the anisotropic flux of particles in the interplanetary medium, and the cap where the flux decrease is observed is determined by the direction of the interplanetary magnetic field [Morfill and Sholer, 1973; Kuznetsov and Tverskaya, 2007]. The existence of anisotropy of solar proton fluxes in the interplanetary medium on 27.08.2022 is confirmed by the results of measuring the pitch-angle distribution of proton fluxes to the L1 point on the WIND spacecraft (Fig. *2b*). It can be seen that a strong pitch-angle anisotropy of proton fluxes was observed at the *L1* libration point from ~ 07 UT to ~ 21 UT on August 27.

Fig. 2.

4. DISCUSSION

The analysis of all solar proton events at 1 a.u. begins with a search for their source on the Sun (sometimes it is absent). However, identical conditions on the Sun (flare coordinates and X-ray score, coronal mass ejection parameters) do not always lead to similar PCA characteristics. The initial acceleration of solar energetic particles occurs on the Sun, but, propagating in the inhomogeneous and unsteady interplanetary medium, the particle streams are affected by large-scale heliospheric structures (see, e.g., [Reames, 2021; Bazilevskaya et al., 2023; Klein and Dalla, 2017]). The study of each individual solar proton event provides an opportunity to expand our

knowledge of the role of the underlying physical processes affecting particle propagation in a variety of interplanetary environments.

Table 1.

The SPS 27.08.2022 (Fig. 1, Table 1), observed at the *L1* libration point and in Earth orbit, has a number of differences from the events associated with sources with similar characteristics (see, for example, [Logachev et al., 2022] and the interactive catalogs of SPSs of the 24th and 25th solar activity cycles (https://swx.sinp.msu.ru/apps/sep_events_cat/index.php?gcm=1&lang= ru)). The temporal profiles of solar proton fluxes from GOES-16 satellite data for the three SPSs on 27.08.2022, 30.03.2022, and 02.04.2022 (within one day for each) are presented in Fig. 3 in one scale, with vertical lines marking the times of solar flares. Table 1 summarizes the parameters of solar flares and coronal mass ejections with which the SPS data are associated. The results of a detailed analysis of the SPS on 30.03.2022 and 02.04.2022 are given in [Vlasova et al., 2024]. It can be seen that the temporal profile of proton fluxes on 27.08.2022 (Fig. *3a*) differs significantly from the profile of 02.04.2022 (Fig. *3c*), whose particle fluxes propagated in a relatively quiet interplanetary medium, but is closer to the profile of 30.03.2022 (Fig. *3b*). On 30.03.2022, the proton fluxes arrived in near-Earth space together with an ICWM formed from two CMEs that emerged from the same AO as the solar protons, but about two days earlier. It was shown in [Vlasova et al., 2024] that the peculiarities of the temporal profile of proton fluxes on 30.03.2022 are caused precisely by the influence of the MCWM.

Fig. 3.

In SPS 27.08.2022, the beginning of the event development followed a similar scenario with SPS 30.03.2022. The source of solar particles on 27.08.2022 is the active region on the Sun No. 13088, in which on the previous day (26.08.2022) several solar flares of X-ray classes C and M, as well as at least two CMEs with sufficiently large velocities and angular solutions having close positional angles (tachymeters) were observed.) several solar flares of X-ray classes C and M were observed, as well as at least two CMEs with sufficiently large velocities and angular solutions that had close positional angles (Table 1, the parameters most important for the study are highlighted in bold). The later but faster CME had to catch up with the earlier one and form a complex MCWM. At the moment of the beginning of the solar flare at 01:52 UT on 27.08.2022, the shock front of the ICWM was at a distance of about 0.2 a.u. from the Sun, and in a few minutes the solar particles should have caught up with the ICWM, which could prevent the direct and rapid arrival of the first particles in near-Earth space. The solar flare on 27.08.2022 was accompanied by its powerful CME. Thus, the solar particle fluxes fell between two shock waves: MCWM2 and MCWM1 (Table 1). In [Bazilevskaya et al., 2025] it is shown that in the event of 27.08.2022 there were particles

accelerated on the Sun, but the main contribution to the proton fluxes with energies above tens of MeV, most likely, was given by the acceleration in the interplanetary medium at distances of 0.2-0.5 a.u. between the approaching fronts of the two CMEs. In the paper, a comparative analysis is made with the results of a study of this event using data from the Parker Solar Probe (PSP) spacecraft, which was at a distance of 0.38 a.u. from the Sun, presented in [Chen and Li, 2024]. The observed more soft spectrum at the particle flux maximum on 27.08.2022 than the spectra at the maxima on 30.03.2022 and 02.04.2022 (Fig. 3) may be the result of proton acceleration between the two MCWMs.

We are interested in the phase of particle flux growth on 27.08.202, namely, the reason for the formation of local maxima without energy dispersion, similar at the *L1* point and at the geostationary orbit, but with delayed arrival in near-Earth space for the time required for the solar wind propagation between these points of space (Fig. 1). The solar particle flux arrived at 1 a.u. at the beginning of the high-speed flux growth (Fig. 4, day 27.08 is marked by a rectangle). The increase in the solar wind density (Fig. *4b*) and the enhancement of the MMP (Fig. *4c*) observed during the phase of the flux velocity growth are characteristic of compression regions in the interaction between fast and slow solar wind fluxes [Richardson, 2018]. The source of the high-speed solar wind flux could be a coronal hole (CH), which passed through the central meridian of the Sun on 21-23.08.2022 (Fig. *4g*). The CD had a complex inhomogeneous structure and was located almost along the solar equator. The high-speed solar wind flux observed from 27.08.2022 could be recurrent, since a similar CD, which passed through the central meridian of the Sun on 26-28.07.2022, was also a source of high-speed flux (not shown).

Fig. 4.

The source of solar energetic particles on August 27 was an explosive process in AO 13088 (Fig. *5a*, left image, the location of AO 13088 is indicated by an oval). At this time, the CD - the source of the high-speed flux– was located at longitudes W50-W80 (Fig. *5a*, right image, the CD is indicated by an oval), which is quite close in longitude to AO 13088. The time profiles of the particle fluxes, as well as the solar wind density and velocity, and the induction and By-component *of* the MMP on 08/27/2022 from satellites located at the *L1* libration point are shown in Fig. 5 (*b*, *c*, *d*, respectively). On the solar wind density and velocity profiles, one can see the alternation of increases and decreases. According to the catalog of large-scale phenomena in the solar wind (http://iki.rssi.ru/pub/omni/), from 04 to 12 UT on 27.08.2022, several shock waves were observed at the *L1* libration point (Fig. 5, vertical dashed lines 1 and 2) and at 12 UT the beginning of the corotating region of interaction of solar wind streams (Fig. 5, vertical dashed line 2). From 08:30 UT to 21:00 UT, a region of strong MMP is observed, mainly due to an increase in the modulus of

the By-component of the MMP directed away from the Sun (Fig. *5g*). The period of the observed solar particle flux anisotropy (Fig. *2b*) coincides with this region of enhanced MMP. However, we cannot speak about the exact time of the beginning of the observation of the particle flux anisotropy because of the small particle fluxes registered both on the WIND spacecraft and on the Meteor-M2 satellite up to~ 08 UT, but the end of the arrival of anisotropic and the beginning of the observation of isotropic fluxes can be determined more precisely: according to the WIND spacecraft data– 21 UT. At the Meteor-M2 satellite, the north-south anisotropy of proton fluxes was observed until about 22 UT (Fig. 5, dashed vertical line 3).

Thus, not only during the growth phase of particle fluxes their spatial distributions are similar at *L1* and with a delay at the geostationary orbit, as can be seen in Figs. *1b* and *1c*, but also the end of the interplanetary structure, determined by the transition from anisotropic to isotropic flux, is fixed at *L1* and in near-Earth space with a delay, which is on average of about 1 h. The time required for the solar wind to travel the distance of 1.5 million km, i.e., between the libration point and near-Earth space, is 70 min. The time required for a solar wind with a speed of 350 km/s to cover a distance of 1.5 million km, i.e., between the libration point and near-Earth space, is 70 min.

Fig. 5.

The results of the study of variations of anisotropic solar particle fluxes observed by the Pioneer 6 spacecraft during 48 hours (30-31.12.1965) made it possible to assume the structured interplanetary medium in the form of magnetic field fibers [McCracken and Ness, 1966; Bartleyr et al., 1966]. At present, more and more evidence is found to support the validity of the representation of the interplanetary medium, at least large-scale interplanetary structures, such as the ICWM and the interaction regions of solar wind flows, as a set of magnetic flux tubes [Borovsky, 2008; Khabarova et al., 2021]. The boundaries separating one tube from another are characterized by rapid changes in the magnitude and direction of the magnetic field [Borovsky, 2018]. Fig. 6 we present the time profiles of proton fluxes on 27.08.2022 using data from the geostationary orbit, while the data on the magnitude of the interplanetary magnetic field components obtained at the *L1* libration point are recalculated to 1 a.u. (https://swx.sinp.msu.ru/tools/ida.php?gcm=1). Assuming that the interplanetary structure arriving at the L1 point on 27.08.2022 consists of similar tubes, we can determine their boundaries from the variations of the IMF components (Fig. 6). The dotted vertical lines in Fig. *6b* are drawn at moments of variation in the magnitude of the MMP components and serve to separate regions with approximately similar dynamics of all three MMP components. All local maxima in the phase

of the solar proton flux accretion (Fig. *6a*) fall into the separated regions quite well. The diameter of the resulting tubes ranges in time from 1 to 2 h, which is equal to (1.2-2.5)· 10^6km at a solar wind speed of 350 km/s on average on 27.08.2022. This is the order of magnitude obtained when estimating the thickness of the tubes in [Bartleyr et al., 1966; Lyubimov et al., 1976; Ermakov et al., 1991], and also the obtained value roughly corresponds to 200 R_E, as suggested in [Borovsky, 2018]. Interestingly, the size of another proposed formation in the solar wind, a magnetic island that crosses 1 a.u. in a time ranging from a few minutes to hours, is estimated to be 10^{-3}-10^{-2} a.u., which is 1.5· 10^5 -1.5· 10^6 km [Khabarova et al., 2021]. It can also be seen that the dashed lines in Fig. *6c* often coincide with rapid changes in the magnitude of the solar wind pressure.

Fig. 6.

Thus, in order to understand the nature and explain the observed features of the SPS on 27.08.2022, we can assume that the region of compression at the interaction of fast and slow solar wind streams has a complex internal structure, which is a set of magnetic flux tubes that is carried at the speed of the solar wind. Cataloged in the catalog of large-scale phenomena in the solar wind (http://iki.rssi.ru/pub/omni/), several shock waves are not pronounced during this period (see Fig. 5). But, probably, it is this formed internal structure of the solar wind flux compression region due to variations in the magnetic field, solar wind density, and velocity that has a modulating effect on the flux of solar particles trapped inside this region and propagating in it. As a result, during the growth phase of the particle fluxes on 27.08.2022, we observe local maxima without dispersion in energy and similarity in the time profiles of proton fluxes at the libration point *L1* and near the Earth, but with a delay corresponding to the time of solar wind propagation between these points, as well as the anisotropy of the particle fluxes for about 12 h. The anisotropy of the particle fluxes is also observed. The anisotropy of solar proton fluxes may be due to the collimating effect in the strong interplanetary magnetic field.

It is known that in the regions of interaction between fast and slow fluxes, the spectrum of solar particles can change: it becomes more rigid in the energy range up to several MeV due to adiabatic cooling and scattering (see, for example, [Fisk and Lee, 1980; Daibog et al., 1981]). However, the hardening of the spectrum is not always observed, and it is insignificant [Allen et al., 2023]. Measurements on several satellites allow to believe that the degree of modulation of particle fluxes depends on the particle path length [Zhao et al., 2016]. The effect of the fast-slow solar wind interaction region is known to affect only the flux of solar particles with energies less than a few MeV and, more often, the electron flux (e.g., [Richardson, 2018; Allen et al., 2023] and references therein).

Experimental data on SPEs show that such an effect as a delay in the arrival of such temporal profiles of solar proton fluxes into near-Earth space compared to the *L1* libration point is not always observed (see the interactive catalogs of SPEs of solar activity cycles 24 and 25 (https://swx.sinp.msu.ru/apps/sep_events_cat/index.php?gcm=1&lang=ru)). At the late stage of a long SPE, the arrival of the coronal mass ejection shock wave, which is one of the sources of the fluxes of these very solar protons, is always accompanied by a small increase in the flux of storm particles, which is first registered at the *L1* point and then, with a delay, in near-Earth space (e.g., [Reames, 2023; Bazilevskaya et al., 2025]). As indicated earlier (see also Fig. 3), a similar pattern of proton flux profile lag to the event of 27.08.2022 was observed in the PCA of 30.03.2022, during which proton fluxes with energies up to 100 MeV are expected to be modulated by an interplanetary coronal mass ejection [Vlasova et al., 2024]. In SPS 27.08.2022, the delayed arrival of the fluxes and the peculiarities of the temporal profile during the growth phase of the particle fluxes are due to the impact of the particle propagation inside the compression region in front of the high-speed solar wind flow from the coronal hole. In the case of the formation of the MCWM, a compression region of fast and slow fluxes is also formed.

There are many unresolved questions in the study of the impact of large-scale heliospheric structures on the solar energetic particle fluxes. In what cases can the effect of delayed arrival of solar particle fluxes be observed, i.e., within which interplanetary structures do the particles propagate? Under what conditions is the observed modulation possible, namely: what should be the ratio between the spatial and temporal distributions of particle fluxes and heliospheric structures? What characteristics must heliospheric structures have in order for a significant modulating effect to be observed as a result of their influence on the solar particle flux? What correspondence exists between the parameters of the solar wind (velocity and density) and the interplanetary magnetic field and the energy of particles whose fluxes have undergone modulation? What are the physical mechanisms that result in the modulation of solar particle fluxes: acceleration, scattering, adiabatic cooling, trapping, or others? These questions are still open, and the answers to them, in our opinion, are very important for understanding the physical processes occurring in the interplanetary medium.

5. CONCLUSION

We present the results of the study of the influence of the state of the interplanetary medium on the propagation of solar energetic particles on 27.08.2022. The solar proton event on 27.08.2022. had an unusual temporal profile of the fluxes of particles with energies up to 30 MeV: simultaneous local maxima of electron and proton fluxes of different energies were observed during the flux growth phase, and the spatial distribution of solar proton fluxes in the near-Earth

orbit was similar to the distribution at the Lagrangian point *L1*, but with a lag of more than 1 h, which corresponds to the time required for the solar wind to overcome 1.5 million km. During the first approximately 12 h of the event, the proton flux was anisotropic. The results of a comparative analysis of the spatial and temporal dynamics of the solar electron and energetic proton fluxes, variations in the density and velocity of the solar wind, and the induction and direction of the interplanetary magnetic field made it possible to conclude that the observed features of the spatial and temporal distribution of the particle flux on 27.08.2022 are due to the modulating effect of the compression region in front of the high-speed solar wind flux from the coronal hole during the propagation of solar particles on their way to Earth inside this region The experimental results obtained do not contradict the assumption about the substructure of the interaction region of fast and slow solar wind streams as a set of magnetic flux tubes.

ACKNOWLEDGEMENTS

The authors are grateful to Yu. S. Shugai for helpful discussion. We thank all researchers who submit their data on proton fluxes and solar wind parameters via the Internet. Experimental data were obtained at NASA's Goddard Space Flight Center: for solar wind and interplanetary magnetic in OMNIWeb– High Resolution OMNI (http://omniweb.gsfc.nasa.gov/form/omni_min.html); for solar proton fluxes in CDAWeb: the Coordinated Data Analysis Web (https://cdaweb.sci.gsfc.nasa.gov). Information on solar flares and coronal mass ejections is obtained from the Coordinated Data Analysis Workshops (CDAW) (https://cdaw.gsfc.nasa.gov), SOHO LASCO CME CATALOG (https://cdaw.gsfc.nasa.gov/CME_list/).

FUNDING

The research was carried out within the framework of the State Assignment of the Lomonosov Moscow State University.

CONFLICT OF INTERESTS

There are no conflicts of interest.

REFERENCES

1. *Bazilevskaya G.A., Vlasova N.A., Ginzburg E.A., Daibog E.I., Kalegaev V.V., Kaportseva K.B., Logachev Yu.I., Myagkova I.N.* Some features of the solar proton event // Proceedings of the Russian Academy of Sciences. Physical series. V. 89. No. 6. 2025 (in print).

2. *Bazilevskaya G.A., Daibog E.I., Logachev Yu.I.* Isolated events of solar cosmic rays caused by the arrival of fast storm particles (ESP) // Geomagnetism and Aeronomy. V. 63. No. 4. P. 503-510. 2023. doi: 10.31857/S0016794023600254

3. *Daibog E.I., Kurt V.G., Stolpovsky V.G.* The spectrum of flare protons in the field of low energies // Space Research. V. 19. No. 5. P. 704-711. 1981.

4. *Ermakov S.I., Kontor N.N., Lyubimov G.P., Tulupov V.I., Chuchkov E.A.* Solar cosmic ray flare in March 1990 // Izvestiya AN SSSR. Physical series. V. 55. No. 10. P. 1889-1893. 1991.

5. Kuznetsov S.N., Tverskaya L.V. Penetration of cosmic rays into the magnetosphere / Model of the cosmos. Vol. 2. Ed. by M.I. Panasyuk, L.S. Novikov. Moscow: KDU. P. 579-591. 2007.

6. *Logachev Yu.I., Bazilevskaya G.A., Vlasova N.A., Ginzburg E.A., Daibog E.I., Ishkov V.N., Lazutin L.L., Nguyen M.D., Surova G.M., Yakovchuk O.S.* Catalog of solar proton events of the 24th solar activity cycle (2009-2019). Moscow: MCD, 970 P. 2022. https://doi.org/10.2205/ESDB-SAD-008

7. *Lyubimov G.P., Kontor N.N., Pereslegina N.V., Ignatiev P.P.* Anisotropy of solar protons and inhomogeneities of the interplanetary medium // Izvestiya AN SSSR. Physical series. V. 40. No. 3. P. 462-470. 1976.

8. *Lyubimov G.P.* Diagnostic methodology for the study of the interplanetary magnetic field, solar wind plasma and their sources in the Sun // Izvestiya AN SSSR. Physical series. V. 67. No. 3. P. 353-366. 2003.

9. *Tverskaya L.V.* Diagnostics of the magnetosphere by relativistic electrons of the outer belt and penetration of solar protons (review) // Geomagnetism and Aeronomy. V. 51. No. 1. P. 8-24. 2011.

10. *Allen R.C., Smith E.J., Anderson B.J. et al.* The solar wind at mesoscales – Revealing the missing link // Bulletin of the American Astronomical Society. V. 55. N 3. ID 008. 2023. https://doi.org/10.3847/25c2cfeb.3e75c979

11. *Bartleyr W.C., Bukata K.P., McCracken K.G., Rao U.R.* Anisotropic cosmic radiation fluxes of solar origin // J. Geophys. Res. V. 71. № 13. P. 3297–3304. 1966. https://doi.org/10.1029/JZ071i013p03297

12. *Borovsky J.E.* Flux tube texture of the solar wind: Strands of the magnetic carpet at 1 AU? // J. Geophys. Res. – Space. V. 113. N 8. ID A08110. 2008. https://doi.org/10.1029/2007JA012684

13. *Borovsky J.E.* The spatial structure of the oncoming solar wind at Earth and the shortcomings of a solar-wind monitor at *L*1 // J. Atmos. Sol.–Terr. Phy. V. 177. P. 2–11. 2018. https://doi.org/10.1016/j.jastp.2017.03.014

14. *Burlaga L., Berdichevsky D., Gopalswamy N., Lepping R., Zurbuchen T.* Merged interaction regions at 1 AU // J. Geophys. Res. – Space. V. 108. № 12. ID 1425. 2003. https://doi.org/10.1029/2003JA010088
15. *Chen X., Li C.* Three-stage acceleration of solar energetic particles detected by Parker Solar Probe // Astrophys. J. Lett. V. 967. № 2. ID L33. 2024. https://doi.org/10.3847/2041-8213/ad4a79
16. *Evans L.C., Stone E.C.* Access of solar protons into polar cap. A persistent north-south asymmetry // J. Geophys. Res. V. 74. № 21. P. 5127–5131. 1969. https://doi.org/10.1029/JA074i021p05127
17. *Fisk L.A., Lee M.A.* Shock acceleration of energetic particles in corotating interaction regions in the solar wind // Astrophys. J. V. 237. P. 620–626. 1980
18. *Klein K.-L., Dalla S*. Acceleration and propagation of solar energetic particles // Space Sci. Rev. V. 212. № 3–4. P. 1107–1136. 2017. https://doi.org/10.1007/s11214-017-0382-4
19. *Khabarova O., Malandraki O., Malova H. et al.* Current sheets, plasmoids and flux ropes in the heliosphere. Part I. 2-D or not 2-D? General and observational Aspects // Space Sci. Rev. V. 217. № 3. ID 38. 2021. https://doi.org/10.1007/s11214-021-00814-x
20. *Mazur J.E., Mason G.M., Dwyer J.R., Giacalone J. Jokipii J.R., Stone E.C.* Interplanetary magnetic field line mixing deduced from impulsive solar flare particles // Astrophys. J. V. 532. № 1. ID L79. 2000. https://doi.org/10.1086/312561
21. *McCracken K.G., Ness N.F.* The collimation of cosmic rays by the interplanetary magnetic field // J. Geophys. Res. V. 71. № 13. P. 3315–3318. 1966. https://doi.org/10.1029/JZ071i013p03315
22. *Morfill G., Scholer M.* Study of the magnetosphere using energetic solar particles // Space Sci. Rev. V. 15. № 2–3. P. 267–353. 1973. https://doi.org/10.1007/BF00169322
23. *Neugebauer M., Giacalone J.* Energetic particles, tangential discontinuities, and solar flux tubes // J. Geophys. Res. – Space. V. 120. № 10. P. 8281–8287. 2015. https://doi.org/10.1002/2015JA021632
24. *Reames D.V.* Solar Energetic Particles. A Modern Primer on Understanding Sources, Acceleration and Propagation. Cham, Switzerland: Springer Nature, 225 p. 2021. https://doi.org/10.1007/978-3-030-66402-2
25. *Reames D.V.* How do shock waves define the space-time structure of gradual solar energetic particle events? // Space Sci. Rev. V. 219. № 1. ID 14. 2023. https://doi.org/10.1007/s11214-023-00959-x

26. *Richardson I.G.* Solar wind stream interaction regions throughout the heliosphere // Living Rev. Sol. Phy. V. 15. № 1. ID 1. 2018. https://doi.org/10.1007/s41116-017-0011-z
27. *Tan L.C., Malandraki O.E., Reames D.V., Ng C.K., Wang L., Dorrian G.* Use of incident and reflected solar particle beams to trace the topology of magnetic clouds // Astrophys. J. V. 750. № 2. ID 146. 2012. https://doi.org/10.1088/0004-637X/750/2/146
28. *Vlasova N.A., Bazilevskaya G.A., Ginzburg E.A., Daibog E.I., Kalegaev V.V., Kaportseva K.B., Logachev Yu.I., Myagkova I.N.* Influence of processes on the Sun and in the interplanetary medium on the solar proton event on March 30, 2022 // Geomagn. Aeronomy. V. 64. № 6. P. 802–813. 2024. https://doi.org/10.1134/S001679322460084X
29. *Zhao L., Li G., Ebert R.W., Dayeh M.A., Desai M.I., Mason G.M., Wu Z., Chen Y.* Modeling transport of energetic particles in corotating interaction regions: A case study // J. Geophys. Res. Space. V. 121. № 1. P. 77–92. 2016. https://doi.org/10.1002/2015JA021762

Table 1. Parameters of solar flares, coronal mass ejections

Solar flares				Coronal mass ejections				ICVM
Date	UT	Coords	Score	UT	*V*, km/s[1]	Δφ, deg [2]	*PA*, deg [3]	
26.08.2022	10:33	S28W55	C2.1	**10:36**	**553**	115	236	MKVM1
26.08.2022	12:52	S27W58	M3.6	**13:36**	**737**	184	266	
27.08.2022	**01:52**	**S17W79**	**M4.8**	**02:24**	**1284**	360	360	MKVM2
30.03.2022	17:21	N13W31	X1.3	17:30	641	360	298	
02.04.2022	12:56	N12W86	M3.9	13:15	1433	360	263	

Note:

1. Median (initial) value of the velocity (*V*, km/s) of the radial propagation of the CME as it moves in the coronograph field of view.
2. Δφ - angular solution (angular width) of the CME near the Sun.
3. *PA* - positional angle of the first appearance of the CME.

FIGURE CAPTIONS

Fig. 1. Time profiles of 27.08.2022:
(*a*) - X-ray fluxes at the wavelength of 0.1-0.8 nm from GOES-16 satellite data;
(*b*) - fluxes of electrons with E=175-315 keV and protons with energies >10 and >30 MeV (from top to bottom) from ACE data;
(*c*) - proton fluxes with energies >5, >10, >30, and >60 MeV (from top to bottom) from GOES-16 data.

Fig. 2. (*a*) Time profiles of proton fluxes with energies 1-100 MeV from Meteor-M2 satellite data and geographic latitude (line) from 08:40 to 09:50 UT on 27.08.2022.
(*b*) Temporal dynamics of the pitch-angle distribution of proton fluxes with energy 6.8 MeV from data of WIND spacecraft on 27.08.2022 (https://cdaweb.gsfc.nasa.gov/).

Fig. 3. Time profiles of proton fluxes with energies >5, >10, >30, >60, >100, and >500 MeV (from top to bottom) from GOES-16 data in 2022: from 00:00 UT 27.08 to 00:00 UT 28.08 (*a*); from 15:30 UT 30.03 to 15:30 UT 31.03 (*b*); from 11:00 UT 02.04 to 11:00 UT 03.04 (*c*). Vertical lines mark the times of solar flares.

Fig. 4. Time profiles of solar wind velocity (*a*) and density (*b*) and MMP induction (c) from DSCOVR satellite data on 25.08-02.09.2022 and composite image of the Sun at wavelengths 193+171+211 Å on 23.08.2022 (*d*).

Fig. 5. Images of the Sun: in soft X-ray emission from Hinode (left) and composite image (211+193+171 Å) from SDO/AIA data (right) (*a*). Time profiles on 27.08.2022: fluxes of electrons with E=175-315 keV and protons with energies >10 MeV and >30 MeV (from top to bottom) from ACE satellite data (*b*); solar wind density and velocity (*c*) and MMP induction and By-component (*d*) from DSCOVR satellite data.

Fig. 6. Time profiles on 27.08.2022: proton fluxes with energies >5, >10, and >30 MeV (from top to bottom) from GOES-16 data (a); *Bx*-, *By*-, and Bz-components *of* the MMP (*b*) and solar wind pressure (*c*) from ACE data, but recalculated to 1 a.u. (see text).

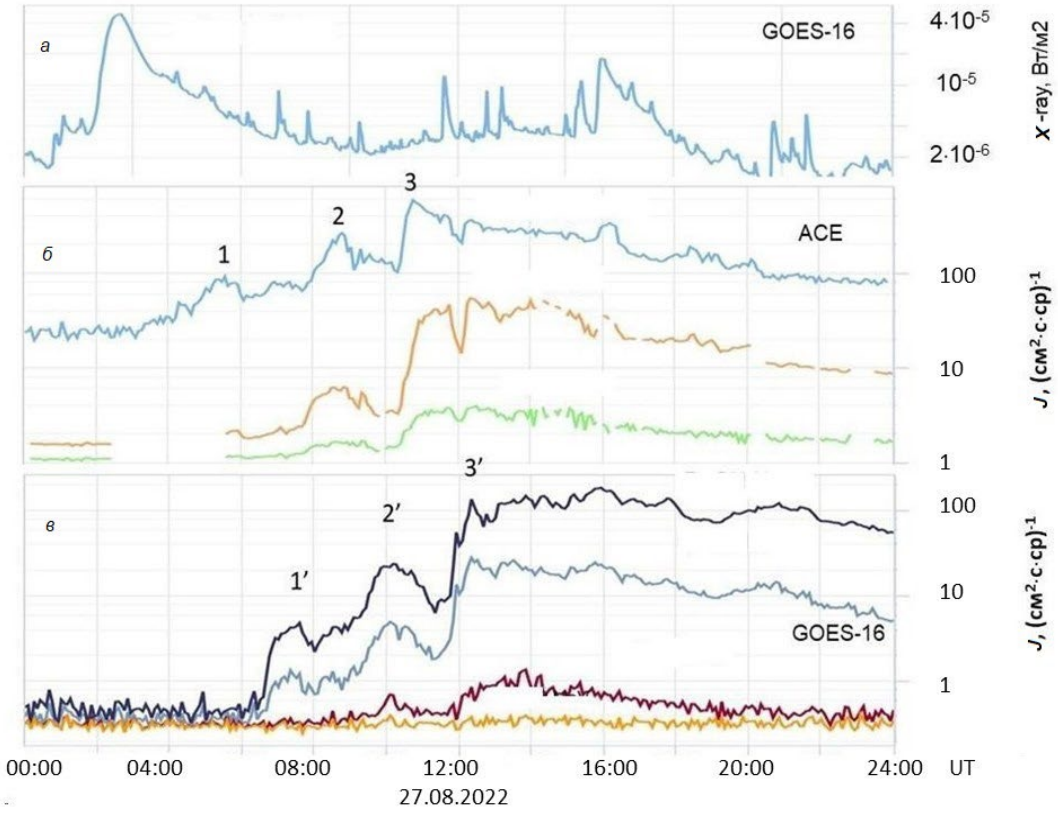
а
GOES-16
4·10-5
10-5
2·10-6
X-ray, Вт/м2
б
ACE
1
2
3
100
10
1
J, (см2·с·ср)-1
в
1′
2′
3′
GOES-16
100
10
1
J, (см2·с·ср)-1
00:00
04:00
08:00
12:00
16:00
20:00
24:00
UT
27.08.2022

Fig. 1.

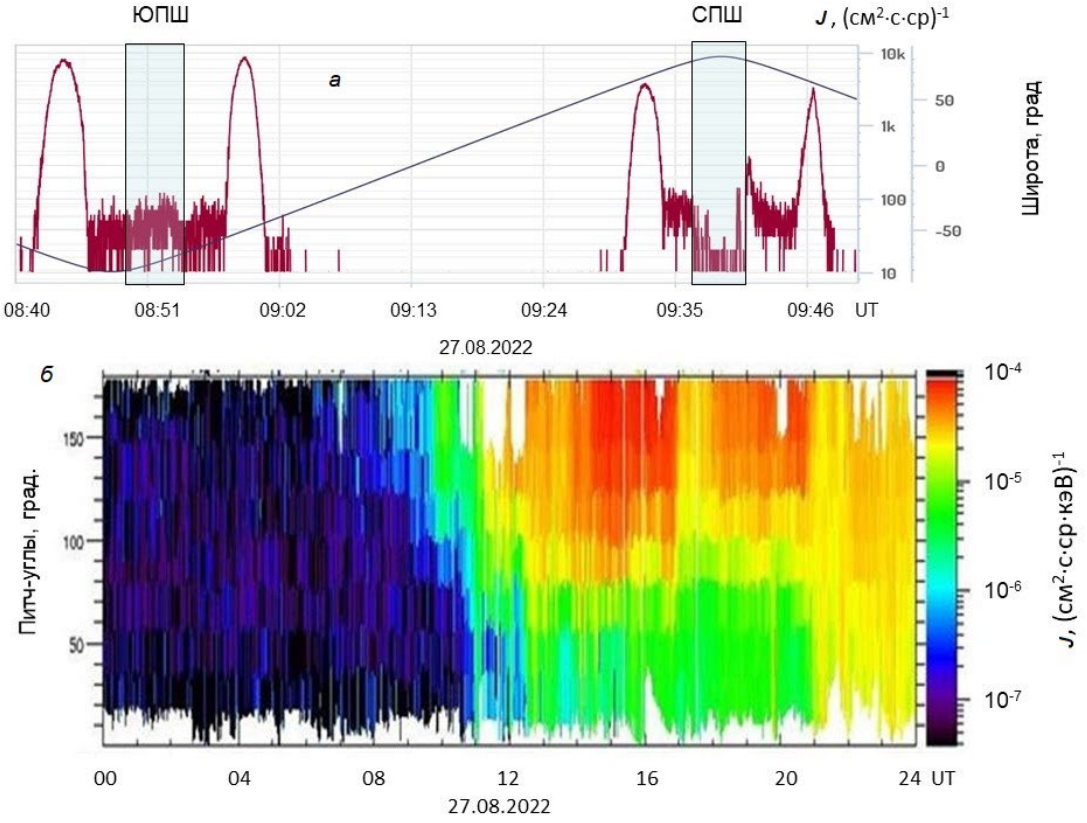
ЮПШ
СПШ
J, (см²·с·ср)⁻¹
а
10k
1k
100
10
50
0
-50
Широта, град
08:40
08:51
09:02
09:13
09:24
09:35
09:46
UT
27.08.2022
б
Питч-углы, град.
150
100
50
10⁻⁴
10⁻⁵
10⁻⁶
10⁻⁷
J, (см²·с·ср·кэВ)⁻¹
00
04
08
12
16
20
24
UT
27.08.2022

Fig. 2.

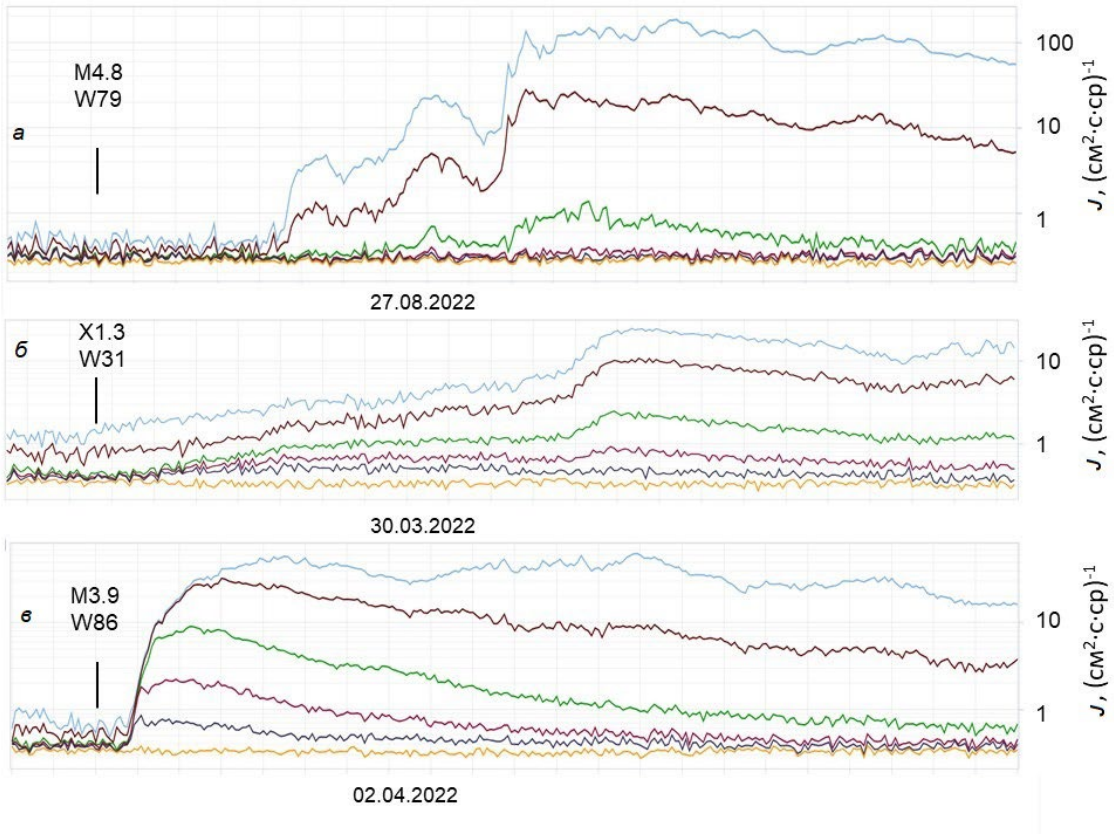
M4.8
W79
а
100
10
1
J, (см²·с·ср)⁻¹
27.08.2022
X1.3
W31
б
10
1
J, (см²·с·ср)⁻¹
30.03.2022
M3.9
W86
в
10
1
J, (см²·с·ср)⁻¹
02.04.2022

Fig. 3.

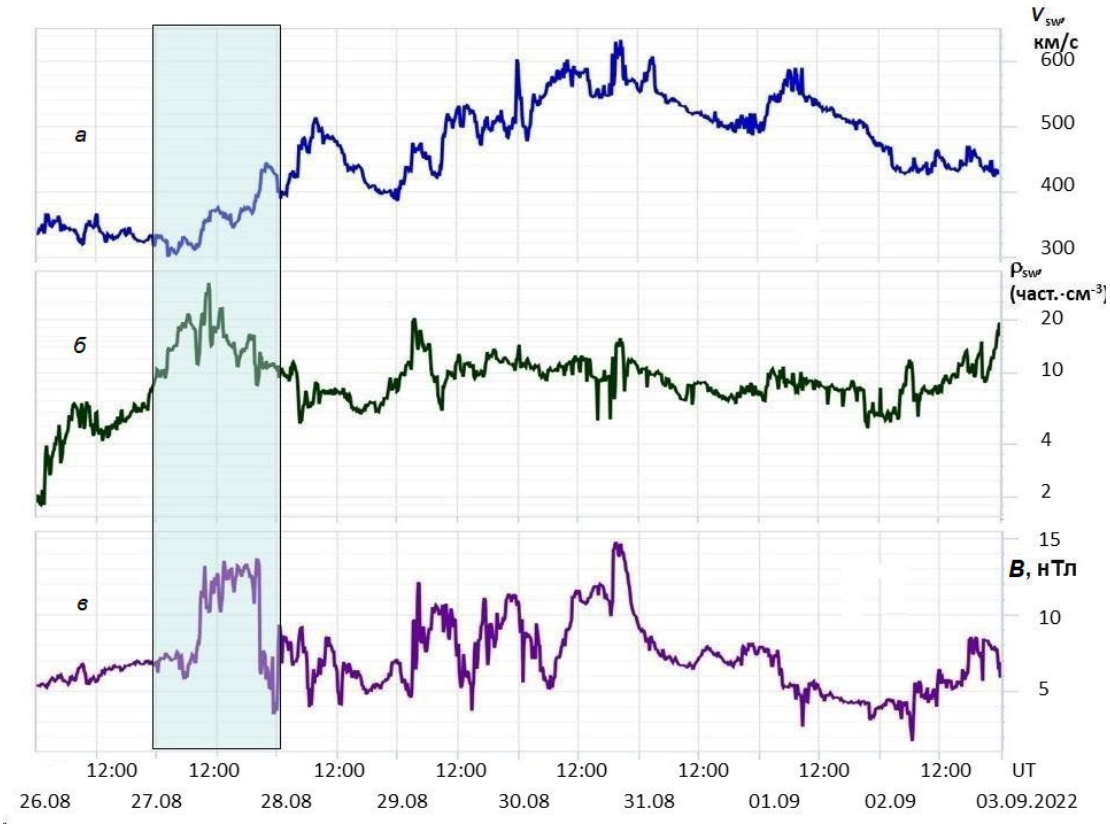
а
б
в
V_{sw}, км/с
600
500
400
300
ρ_{sw}, (част.·см$^{-3}$)
20
10
4
2
15
B, нТл
10
5
12:00
26.08
27.08
28.08
29.08
30.08
31.08
01.09
02.09
03.09.2022
UT

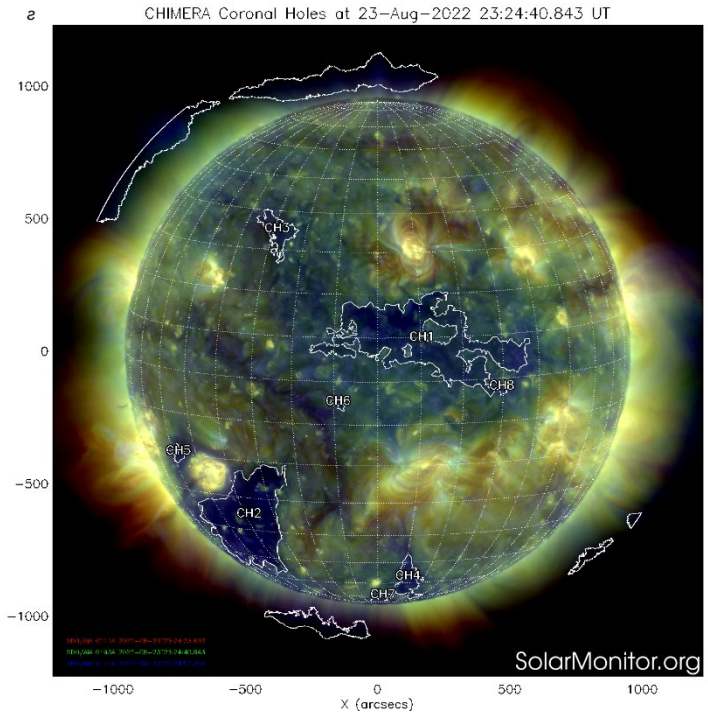
г
CHIMERA Coronal Holes at 23–Aug–2022 23:24:40.843 UT
CH5
CH1
CH8
CH6
CH5
CH2
CH4
CH7
SolarMonitor.org
1000
500
0
−500
−1000
X (arcsecs)

Fig. 4.

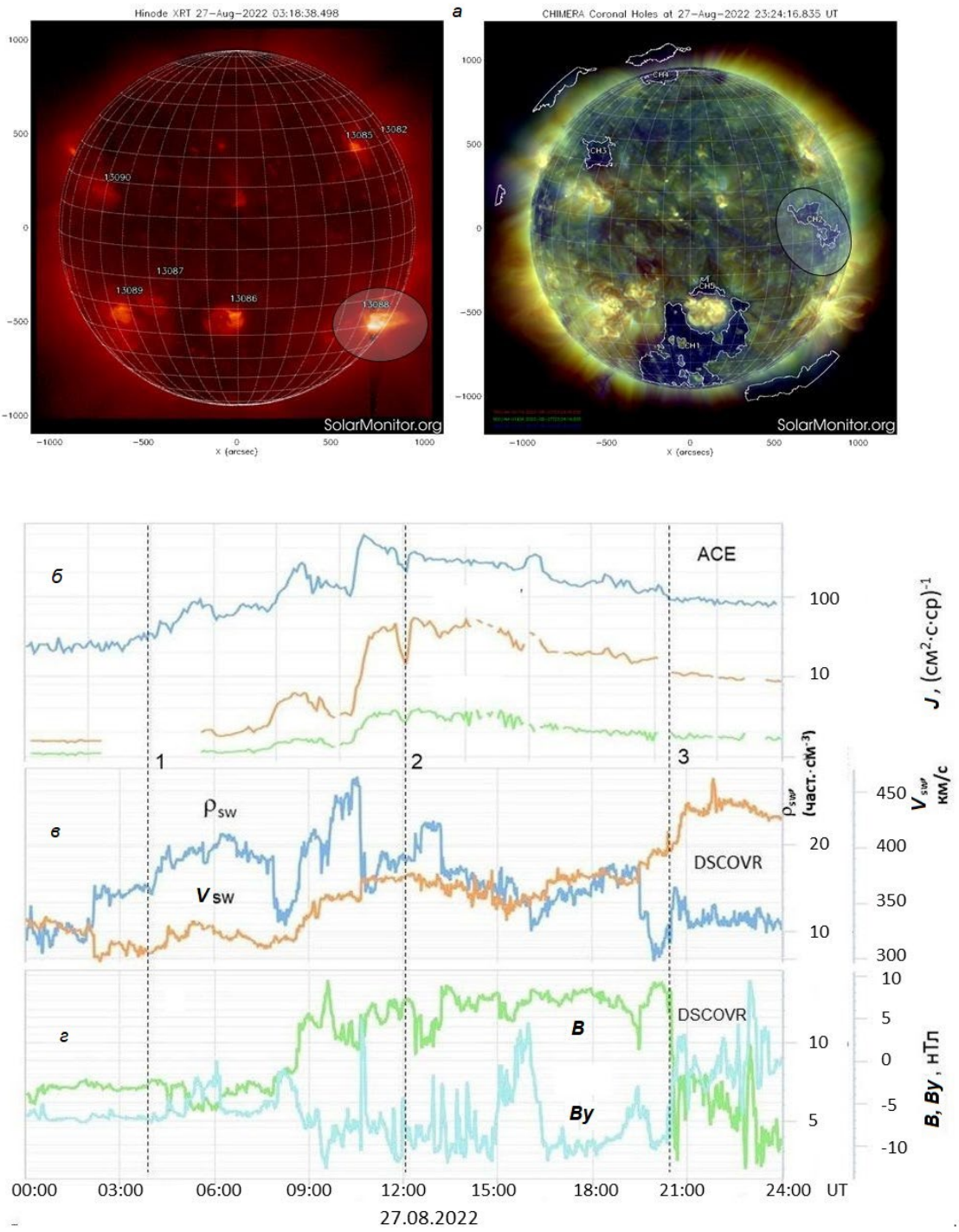
Hinode XRT 27-Aug-2022 03:18:38.498
13090
13085
13082
13087
13089
13086
13088
SolarMonitor.org
X (arcsec)
а
CHIMERA Coronal Holes at 27-Aug-2022 23:24:16.835 UT
CH4
CH3
CH2
CH5
CH1
SolarMonitor.org
X (arcsecs)
б
ACE
J, (см²·с·ср)⁻¹
1
2
3
в
ρsw
Vsw
DSCOVR
ρsw, (част.·см⁻³)
Vsw, км/с
г
B
By
DSCOVR
B, By, нТл
00:00
03:00
06:00
09:00
12:00
15:00
18:00
21:00
24:00 UT
27.08.2022

Fig. 5.

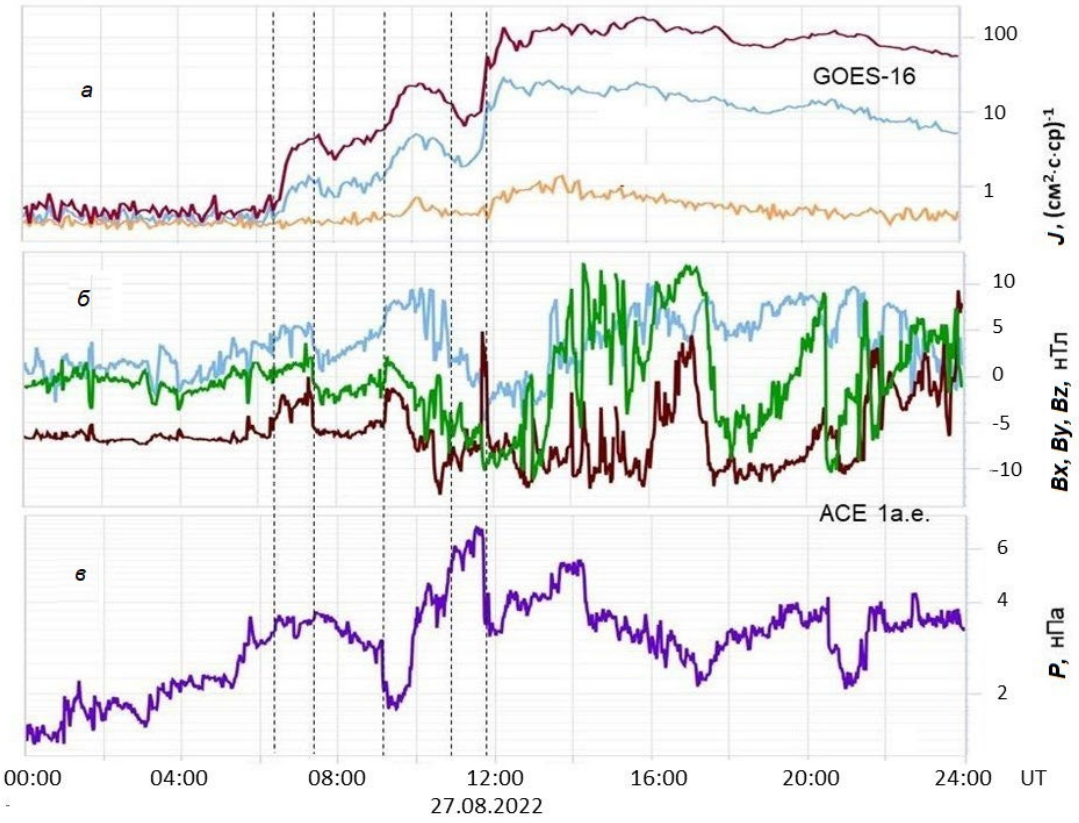
а
GOES-16
100
10
1
J, (см²·с·ср)⁻¹
б
10
5
0
-5
-10
Bx, By, Bz, нТл
ACE 1a.e.
в
6
4
2
P, нПа
00:00
04:00
08:00
12:00
16:00
20:00
24:00
UT
27.08.2022

Fig. 6.